

***In-situ* incorporation of Cobalt Nanocluster and Nitrogen into Carbon matrix: a bifunctional catalyst for the oxygen depolarized cathode and chlorine evolution in HCl electrolysis**

Vikram Singh and Tharamani C. Nagaiah*

Department of Chemistry, Indian Institute of Technology Ropar, Rupnagar, Punjab-140001, India

Experimental Section

Materials

The cobalt nitrate ($\text{Co}(\text{NO}_3)_2 \cdot 6\text{H}_2\text{O}$; $\geq 98\%$), dimethylglyoxime and diethylamine procured from Alfa Aesar ethanol ($\geq 99\%$) from Merck Millipore. All the chemicals are of analytical grade without further purification. The required solutions were prepared using Millipore water (15 M Ω).

Synthesis of Cobalt oxime complex.

The Cobalt-oxime complex was synthesized using reported procedure.¹ Briefly, 4 mmol of dimethylglyoxime (DMG) was dissolved in 60 ml of boiling ethanol. The 20 ml aqueous solution containing 2 mmol of cobalt nitrate was separately prepared and followed by addition to dimethylglyoxime solution under vigorous stirring. After continuous stirring for one hour 4 mmol of secondary ligand *i.e.* diethyl amine was added. Precipitates were obtained within the refluxing time for the complex and the precipitated product were washed multiple times using mixture of ethanol and water (1:3) and dried for overnight at room temperature.

Synthesis of Cobalt nanocluster and nitrogen incorporated carbon *i.e.* Co-NSC

The co-insertion of both Cobalt and nitrogen into the carbon matrix was synthesized by pyrolyzing the above as such obtained Co-oxime complex without the utilization of external soft or hard template by treating at various temperature such as 600, 800 and 900 °C under inert atmosphere (Ar, 25 sccm) at a heating rate of 5 °C per minutes for 2 h. Depending upon the pyrolysis temperature, the obtained product were subsequently termed as Co-NSC6, Co-NSC8 and Co-NSC9 upon treating the sample at 600, 800 and 900 °C respectively.

Physical characterization

The physical characterization of synthesized cobalt nanocluster and nitrogen incorporation in carbon matrix were investigated using powder X-ray diffraction (PXRD) measurements in the 2θ range from 10 to 70 degree using PANalytical's X'Pert Pro MPD wherein the X-ray source was Cu K α radiation. The morphology of each variant were analyzed using field emission electron microscopy (FE-SEM) ZEISS, ULTRA PLUS. The elemental composition was analyzed using energy dispersive X-ray spectroscopic measurements (EDS; Oxford, INCAx-act, 51-ADD0013). The nitrogen content in the each variants *i.e.* Co-NSC6, Co-NSC8 and Co-NSC9 were determined by performing CHNS analysis FlashSmart™ Elemental Analyzer from Thermo Scientific. The Cobalt content was analyzed in each variants by performing MP-AES measurements by dissolving the obtained sample in 2-4% nitric acid solution. Further, both nitrogen and cobalt doping in the carbon matrix was confirmed by performing X-ray photoelectron spectroscopy (XPS; PHI Versa Probe II Spectrometer) working at 15 kV under an ultrahigh vacuum (UHV; 7×10^{-10} mbar) using Al K α monochromatic radiation ($h\nu = 1486.6$ eV). The measurements were performed in fixed transmission

mode with a pass energy of 376 eV to obtain Co 2p, S 2p and C 1s spectra. The obtained spectra were calibrated w.r.t to C1s. The FT-IR measurements were performed using Bruker Tensor-27 spectrometer in the frequency range of 400–4000 cm^{-1} , with a spectral resolution of 4 cm^{-1} run by OPUS software.

Electrochemical Measurements

Sample preparation and electrochemical analysis

Glassy carbon electrode served as working electrode in the present study and was cleaned prior to each measurement by employing different grades of alumina slurry (3, 0.3, 0.05 μm PINE instrument, USA) on the nylon polishing cloths (SM 407052, AKPOLISH). Further, the working electrodes were prepared by drop casting 20 μl of prepared slurry on glassy carbon electrode (\varnothing 3mm). The slurry was prepared for each catalyst by adding 40 μl of isopropanol (IPA) in the 2.5mg of catalyst. The obtained dispersion was continuously sonicated till homogenized, followed by addition of 960 μl of water and again sonicated for next 1 h till the solution mixture is completely homogenous. Further, the electrochemical measurements were performed using Autolab 302N modular potentiostat/galvanostat connected with Nova 1.11 software. The electrochemical measurements were carried out using three-electrode assembly, which was comprised of working electrode (a glassy carbon electrode coated with catalyst), Ag/AgCl/3M KCl as reference electrode and Pt-mesh was employed as counter electrode. The working electrode was prepared by drop-casting 20 μl of catalyst slurry followed by drying at room temperature. The RDE measurement were performed for each variants by sweeping the potential from 1.2 V to 0.0 V in the oxygen saturated 0.4 M HCl solution. For the better comparison, same amount of noble metal based catalyst such as Pt/C (20%, purchased from E-TAK), RhxSy/C (30%, BASF) and $\text{RuO}_2/\text{TiO}_2$ (synthesised) were also casted over the same GC and performed their analysis under the similar conditions.

The electrochemical impedance measurements were recorded in the 0.4 M HCl solution using 5 mM of $\text{K}_4[\text{Fe}(\text{CN})_6]$ redox media. The impedance measurement was performed by applying a DC potential of 325 mV over and above AC perturbation of 20 mV for the various frequency ranging from 10Hz to 200 kHz in the logarithmic steps.

Scanning electrochemical studies

The local electrocatalytic activity and distribution of active sites over the catalyst spot was investigated using scanning electrochemical microscopic (SECM) technique. The SECM analysis were recorded using Sensolytics Base SECM (Sensolytics, Bochum, Germany) with stepper-motor-driven x-y-z stages and an additional three axis piezo-positioning system working in conjunction with the bi-potentiostat (Autolab 204, Metrohm). In order to perform the SECM measurements, four electrodes assembly were employed which includes Pt- micro-electrode (WE2) having diameter of 10 μm , Ag/AgCl/3M KCl as reference, Pt-coil as counter and glassy carbon plate containing catalyst spot were served as working electrode (WE1) respectively in oxygen saturated 0.4 M HCl solution. The redox competitive mode of SECM was employed to measure the electrocatalytic ability of each sample vs. Pt-microelectrode towards oxygen reduction in 0.4 M HCl solution. Both the electrode were continuously polarized at their respective diffusion limiting potential. The array scan was performed in 2000 $\mu\text{m} \times 2000 \mu\text{m}$ area, with increment of 10 μm in X-direction and 20 μm in Y-direction using tile-control mode. The obtained data were collected and further analyzed using Gwydion and origin 8.5 software.

➤ **Rotating ring-disk Analysis:**

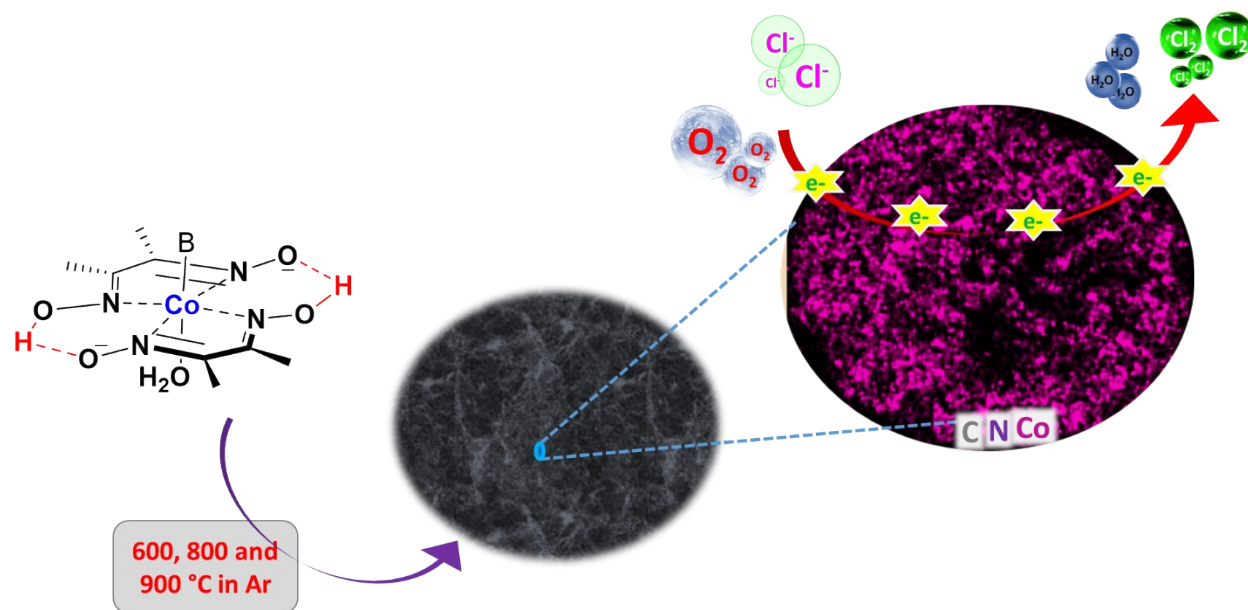
The rotating ring-disk electrode measurements we performed for each variants in oxygen saturated 0.4 M HCl solution in the potential range of 1.1 V to -0.1 V at a scan rate of 5 mV/s using gold ring embedded in the Teflon lined GC at various rotation speed ranging form 100 rpm to 1300 rpm. The collected RRDE polarization was further used to calculate the percentage of H₂O₂ formation along with number of electrons transferred during the electroatalytic reduction of oxygen using following equation;

$$n = 4I_d \left[I_d + \left(\frac{I_r}{N} \right) \right]$$

Where 'I_d' and 'I_r' represents the disk and ring current collected during ORR. Whereas, N stands for collection efficiency of ring determined to 0.38 by performing RRDE analysis in Fe^{2+/3+} redox medium

The percentage of peroxide formation was also evaluated using the following equation;

$$\% \text{H}_2\text{O}_2 = 200 \times (I_r/N) / [I_d + (I_r/N)]$$



Scheme S1. Schematic representation of synthesis of Co-NSCt (t= various temperature) under inert atmosphere of argon and its expected activity under HCl electrolysis conditions.

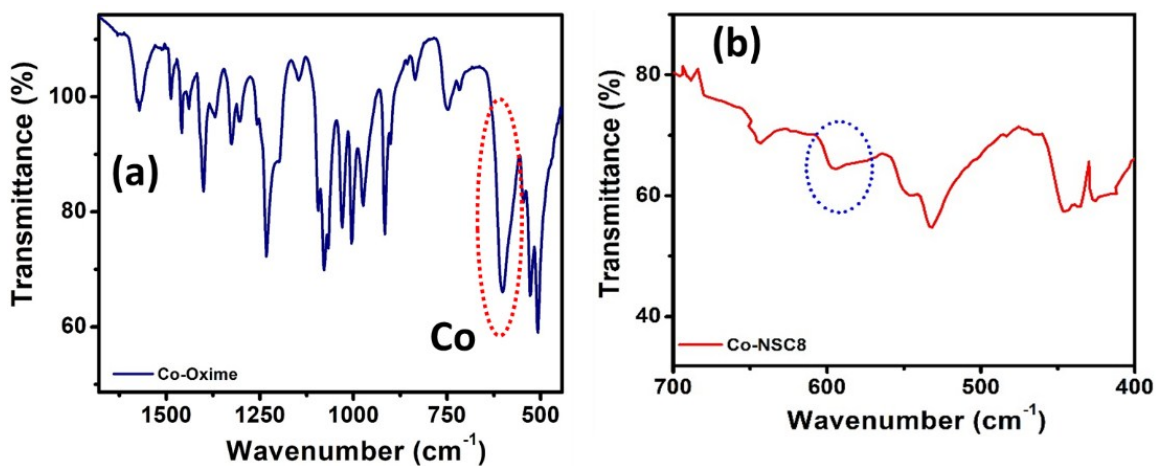


Figure S1. FT-IR spectra of as synthesized (a) Co-oxime complex and (b) Co-NSC8 catalyst shows the presence of Cobalt.

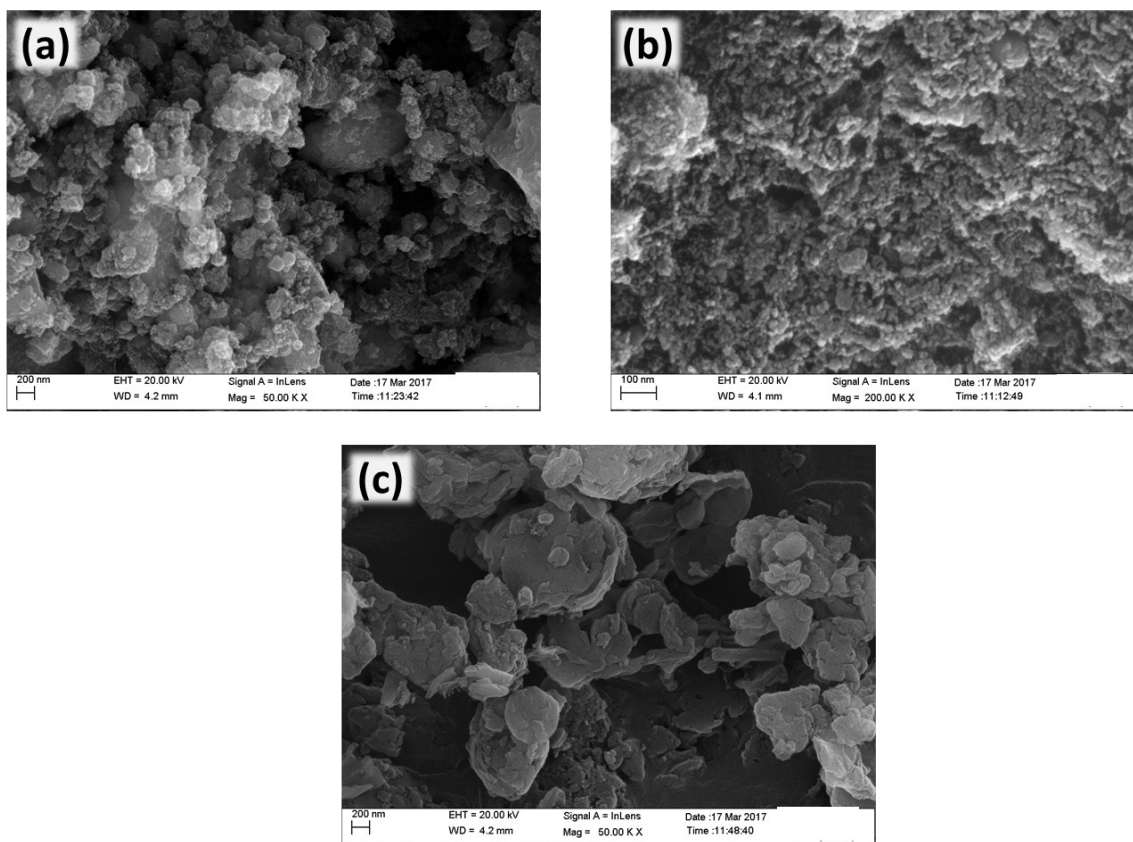


Figure S2. FE-SEM image of (a) Co-NSC6, (b) Co-NSC8 and (c) Co-NSC9

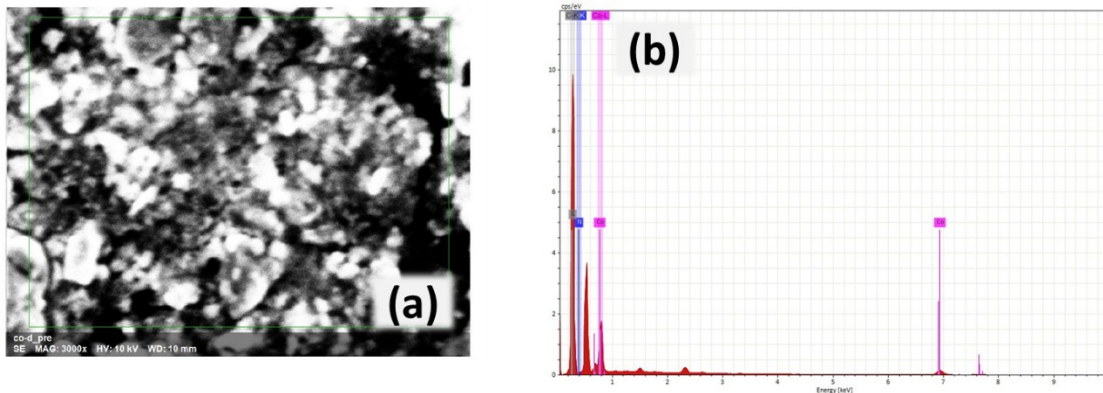


Figure S3. EDS spectra of Co-NSC8 shows the presence of respective elements over scanned area.

Table S1: EDS and CHNS/O (%)						
Sample	Carbon		Nitrogen		Cobalt	
	EDS	CHNS/O	EDS	CHNS/O	EDS	CHNS/O
Co-NSC6	80.8	90.8	8.2	9.2	8.3	-
Co-NSC8	94.1	97.4	2.9	2.3	1.2	-
Co-NSC9	95.5	98.1	2.1	1.8	1.4	-

Table S2: MP-AES analysis (ppm)	
Sample	Co (ppm)
Co-NSC6	15.23
Co-NSC8	10.35
Co-NSC9	9.83

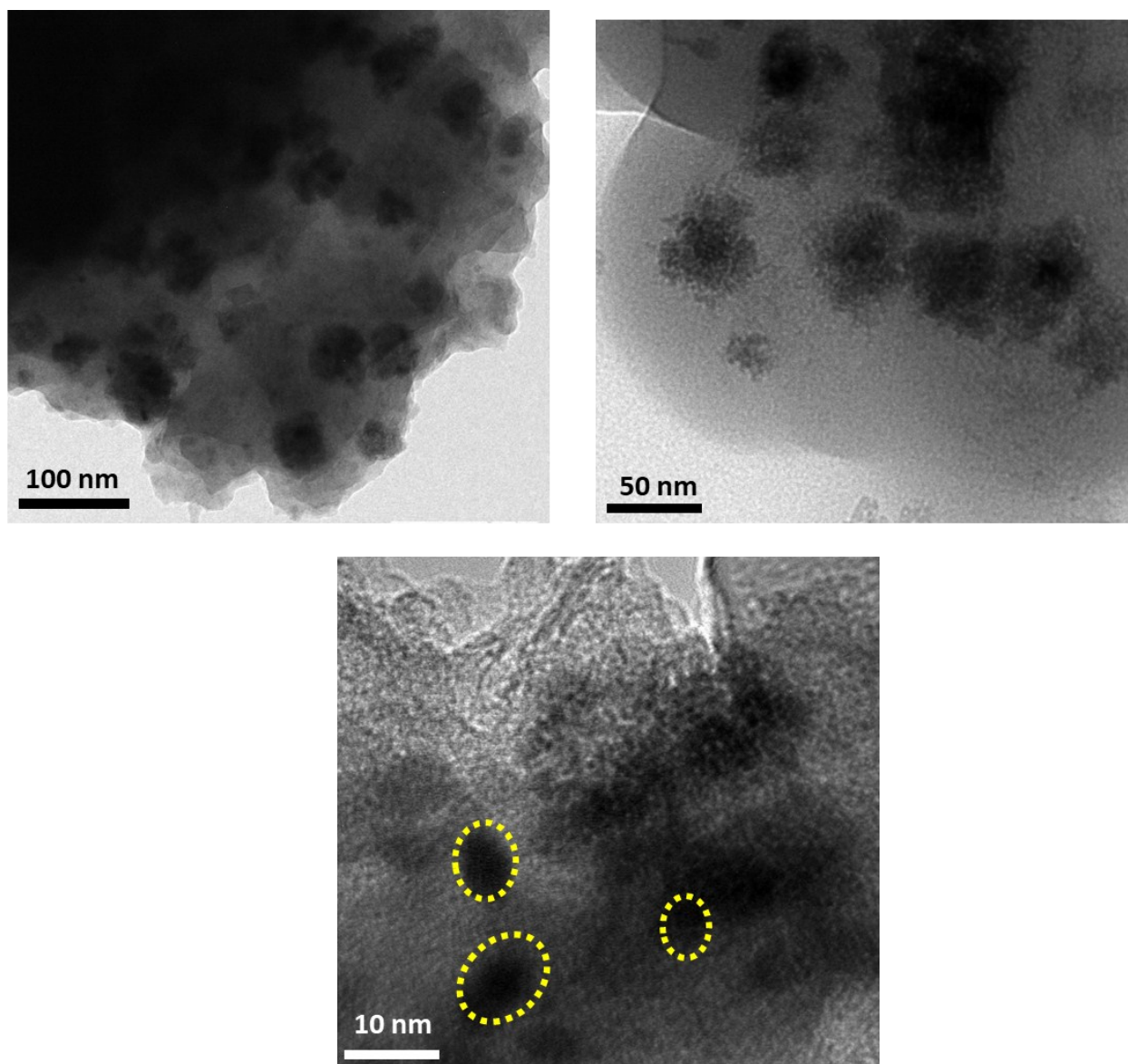


Figure S4. TEM and HR-TEM images of Co-NSC8 catalyst at different magnification.

Table S3: XPS analysis (%)				
Sample	C	N	Co	O
Co-NSC8	93.1	4.7	2.2	<1
Co-NSC9	93.7	4.2	2.1	<1

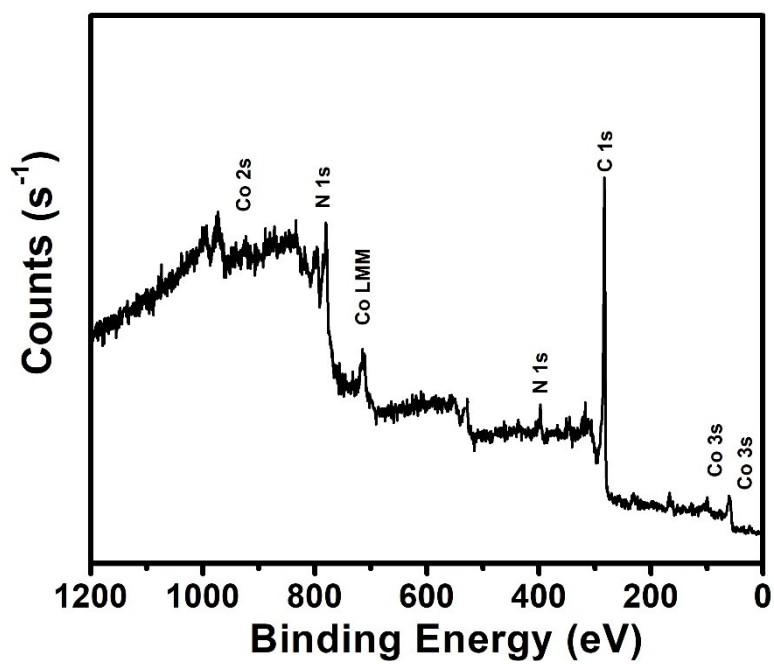


Figure S5. XPS survey spectra of Co-NSC8 catalyst.

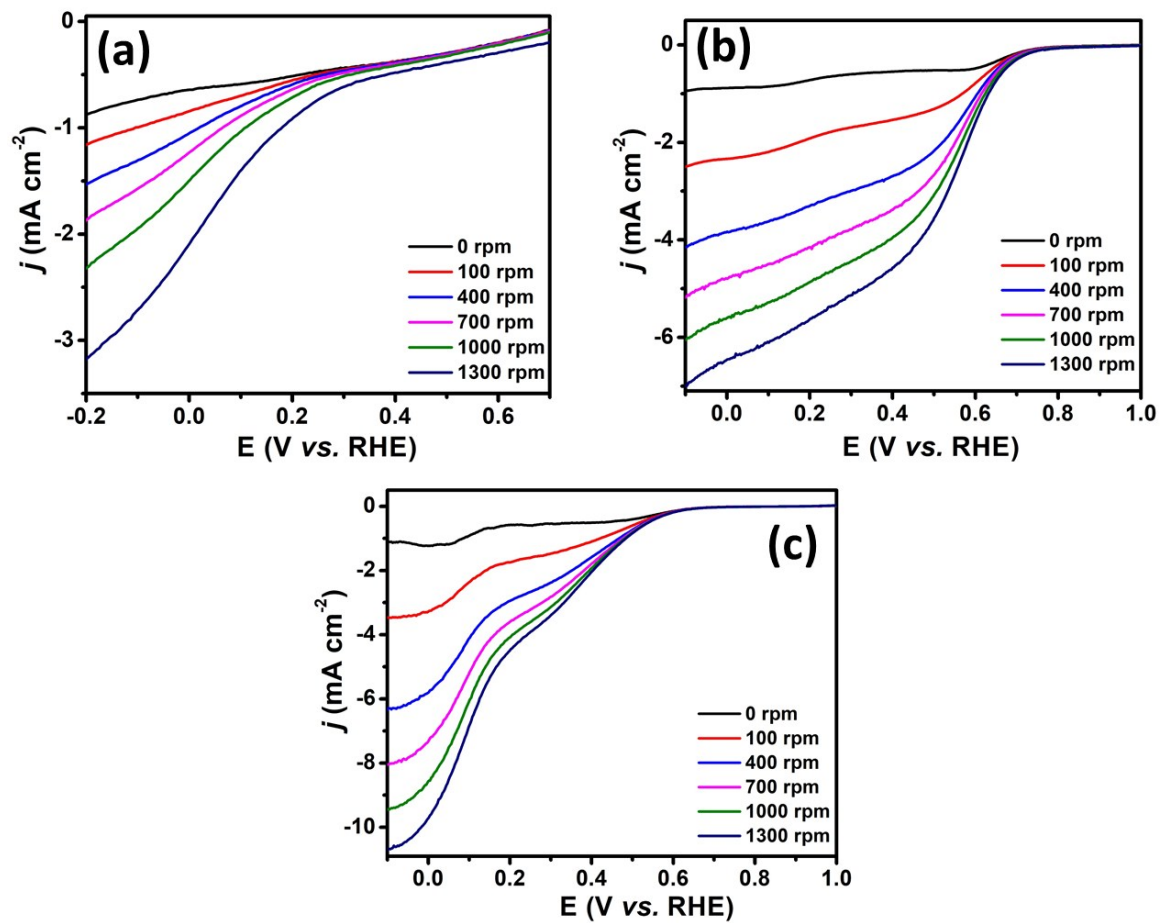


Figure S6. Linear sweep polarization curve obtained at various rotation speed (0 rpm to 1300 rpm) for (a) Co-NSC6, (b) Co-NSC8 and (c) Co-NSC9 at a scan rate of 5 mVs⁻¹ in oxygen saturated 0.4 M HCl solution. RE Ag/AgCl (potential are converted to RHE), CE; Pt-mess.

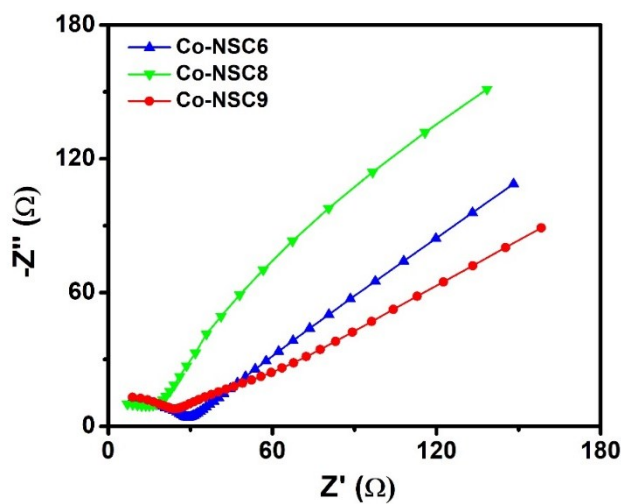


Figure S7. Electrochemical impedance spectroscopy measurements collected for each variants in the 5 mM of $K_4[Fe(CN)_6]$ in 0.4 M HCl solution.

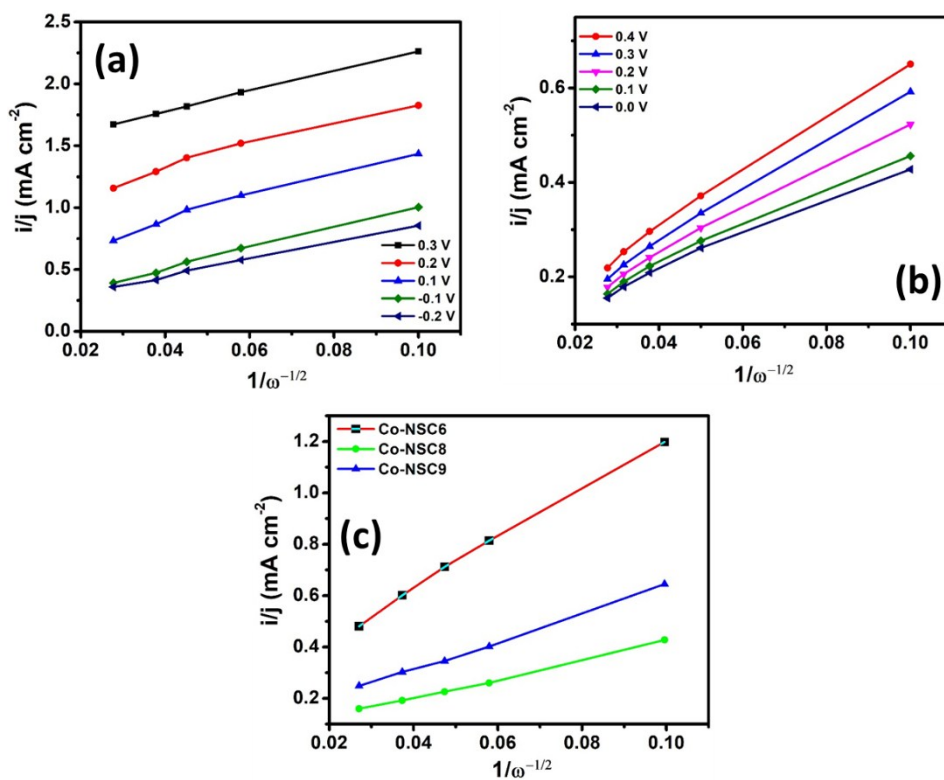


Figure S8. Potential dependent K-L plot for (a) Co-NSC6, (b) Co-NSC8 and (c) a comparative K-L plot for all the variants at 0.4 V (vs. RHE) extracted from polarization curve shown in figure S3.

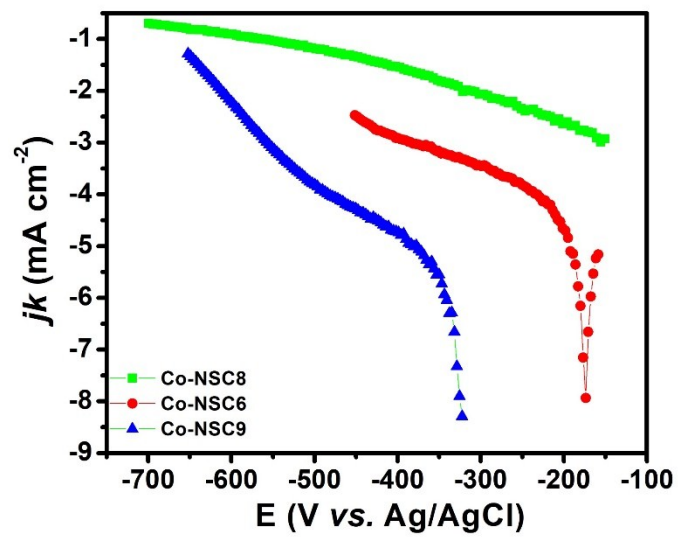


Figure S9. Tafel-plot for all variants at a potential of 0.1 V (vs.RHE) and extracted from figure S3.

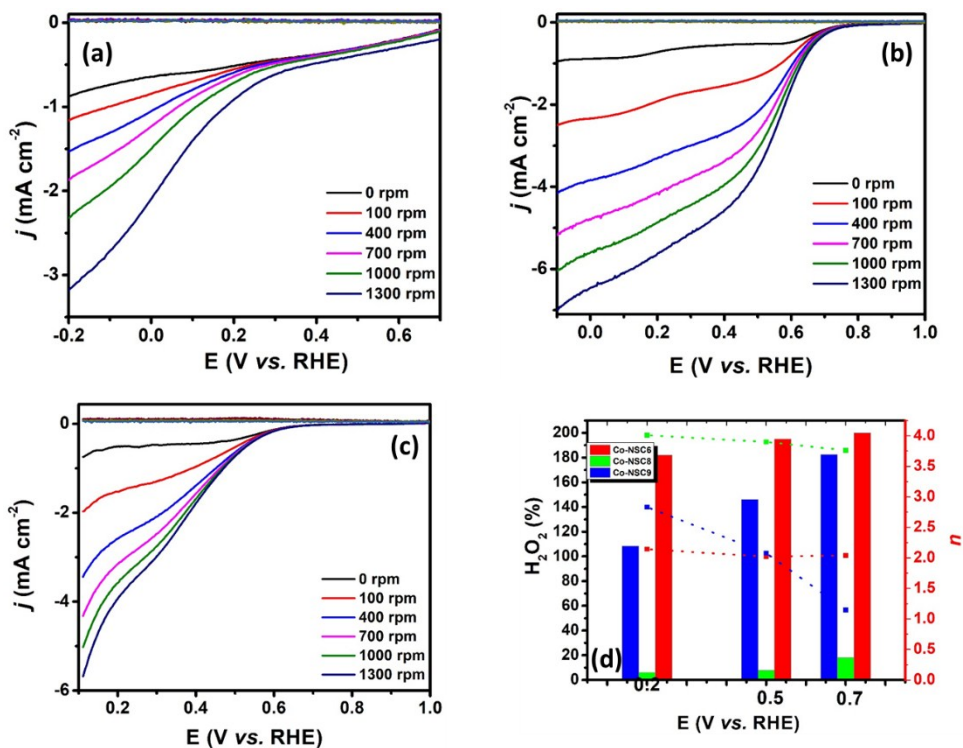


Figure S10. Rotating ring disk electrode (RRDE) analysis collected for each variants (a) Co-NSC6, (b) Co-NSC8 and (Co-NSC9) respectively in oxygen saturated 0.4 M HCl at various rotation speed ranging from 0 to 1300 rpm. (d) Represents the percentage of H₂O₂ collected at the gold ring along with number of electrons transferred at various potential for each variants, (d) extracted from the RRDE polarization curve from (a-b). CE, Pt-wire, RE, Ag/AgCl.

Electrochemical surface area analysis

The electrochemical active surface area (ESCA) was determined for each variants such as Co-NSC6, Co-NSC8 and Co-NSC9 by evaluating double-layer capacitance (C_{dl}) measurements. In order to find out the C_{dl} cyclic voltammograms were recorded at various scan rate in the range of 10 mV/s to 320 mV/s in the non-faradaic potential region (in the present case 0.0 to -0.2V) in 0.4 M HCl solution. Further, the obtained response was therefore attributed to have the origin only in the capacitance behavior of the electrolytic

system. A plot were plotted for each catalyst between the average current density $(I_a+I_c/2)$; where I_a represents the anodic current and I_c for cathodic current at -0.1 V (vs. Ag/AgCl) vs. scan rate which results in a linear graph with the slop of which give the double-layer pseudo-capacitance (C_{dl}). Further, upon

dividing obtained C_{dl} value with specific capacitance for a plane surface ($40 \times 10^{-6} \text{ F cm}^{-2}$)^{2, 3} yields ECSA to be 19.8 cm².

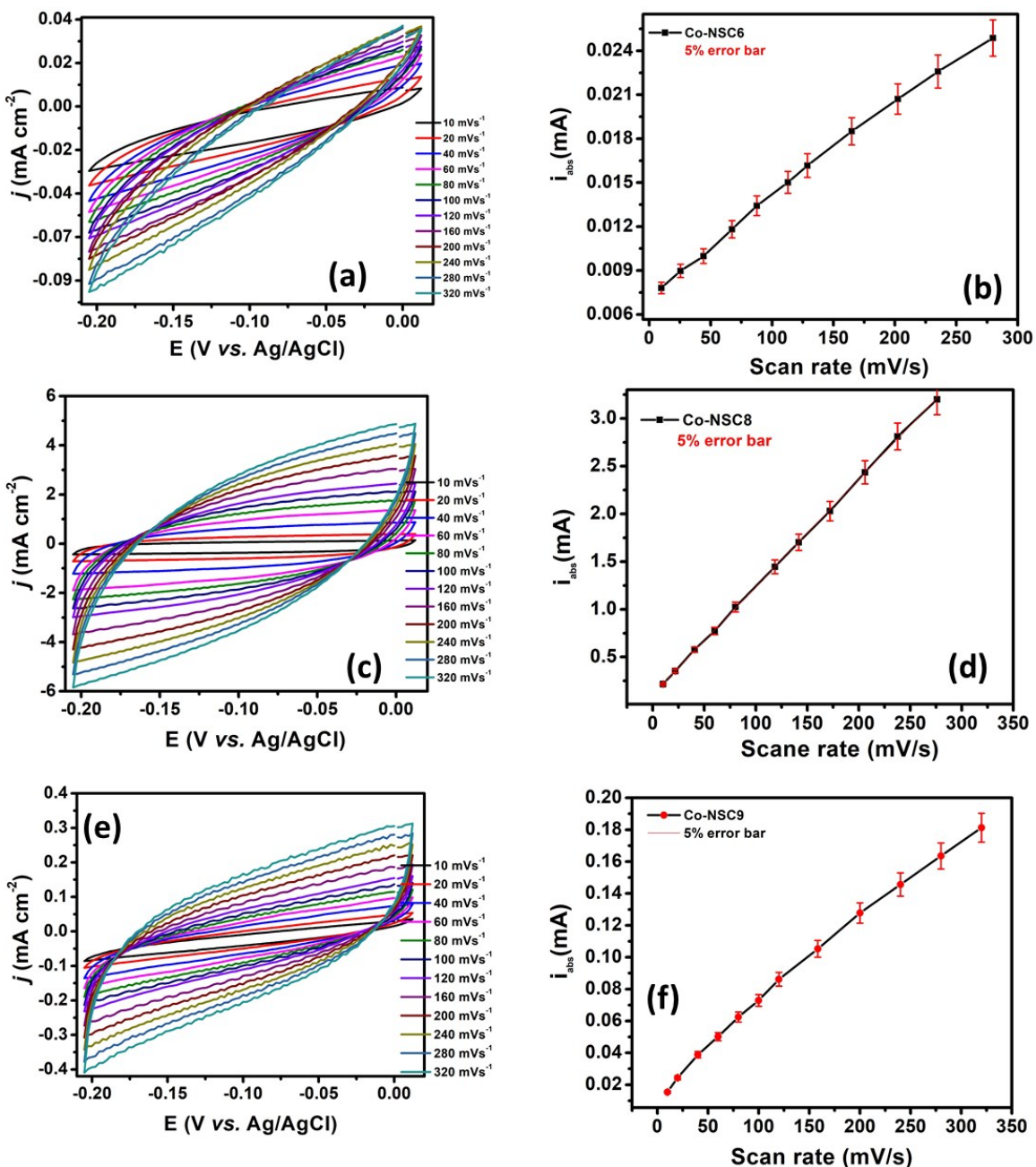


Figure S11. Cyclic voltammogram in the non-faradic potential region at varying scan rates (10 mVs⁻¹ to 320 mVs⁻¹) and the corresponding plot of average current density vs. scan rate for all the variants Co-NSC6, Co-NSC8 and Co-NSC9 respectively in 0.4 M HCl electrolyte solution. CE: Pt-mesh; RE: Ag/AgCl/3 M KCl

Table S4. ESCA Measurements		
Catalyst	ESCA (cm ²)	Specific Surface area (m ² /g)
Co-NSC6	0.11	0.22
Co-NSC8	19.8	39.6
Co-NSC9	0.93	1.86

Turn over frequency calculation:⁴

$$\text{TOF} = \frac{\# \text{ total water/Cl}_2 \text{ turnover / cm}^2 \text{ geometrical area}}{\# \text{ surface sites / cm}^2 \text{ geometrical area}}$$

Total number of water during the oxygen reduction (cathodic process) and Cl₂ evolution while oxidation of HCl (anodic process) turn overs number can be calculated using current density as stated below;

$$\begin{aligned} \text{H}_2\text{O/Cl}_2 &= j \left(\frac{\text{mA}}{\text{cm}^2} \right) \left(\frac{1 \text{ Cs}^{-1}}{1000 \text{ mA}} \right) \left(\frac{1 \text{ mol of } e^-}{96500 \text{ C}} \right) \left(\frac{1 \text{ mol of H}_2\text{O/Cl}_2}{2 \text{ mol of } e^-} \right) \left(\frac{6.022 \times 10^{23}}{1 \text{ mol of H}_2\text{O/Cl}_2} \right) \\ &= 3.12 * 10^{15} \frac{\text{H}_2\text{O/Cl}_2 \text{ per sec}}{\text{cm}^2} \text{ per mA/cm}^2 \end{aligned}$$

The number of active site in all the Co-NSC samples were evaluated from the mass loading of catalyst over glassy carbon electrode by assuming that only Co-center is responsible for activity and each cobalt site is equivalent to one active site. The Cobalt content and Co atomic weight was considered to calculate the active sites.

$$\begin{aligned} \# \text{ active sites} &= \left(\frac{\text{Catalyst loading per geometric area} \left(x \frac{\text{g}}{\text{cm}^2} \right) * \text{Co wt}\%}{\text{Co } M_w \left(\frac{\text{g}}{\text{mol}} \right)} \right) * \left(\frac{6.023 * 10^{23} \text{ Co atoms}}{1 \text{ mol of Cobalt}} \right) \\ &= \frac{0.707 * 10^{-3} \frac{\text{g}}{\text{cm}^2} * 2.2 \text{ wt}\%}{58.93 \text{ g/mol}} * \left(\frac{6.023 * 10^{23} \text{ Co atoms}}{1 \text{ mol of Cobalt}} \right) \\ &= 1.5 * 10^{17} \text{ Cobalt sites per cm}^2 \end{aligned}$$

Finally, TOF can be evaluated by putting these values along with the current density taken from polarization curve of LSV as accordingly.

$$\text{TOF} = \left(\frac{3.12 * 10^{15}}{1.5 * 10^{17}} * j \right) = 0.0204 * j$$

For the better comparison, TOF for Rh_xS_y/C was also evaluated and compared with Co-NSC8 considering 30 wt% of Rh₃S₄ in Rh_xS_y/C.⁵

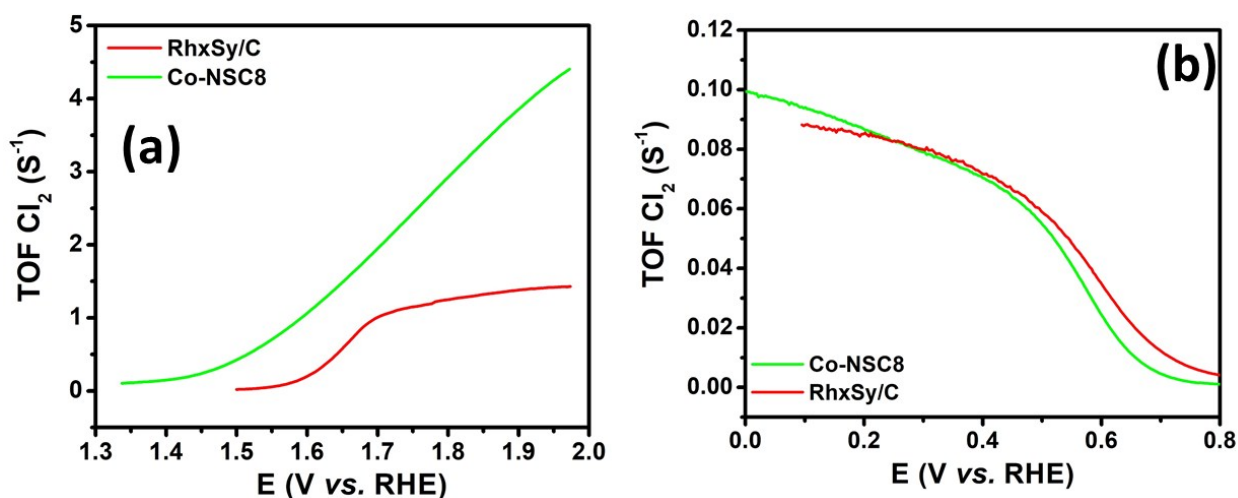


Figure S12. Potential dependent TOF for (a) chlorine evolution and (b) ORR for both Co-NSC8 and Rh_xS_y/C.

Determination of Cl₂ evolution by Iodometric titration:

The amount of chlorine gas evolved for each variant after 50 seconds of continuous HCl oxidation at 1.5 V in 0.4 M HCl in vertical aligned airtight glass vial. The obtained chlorine gas was further trapped by immediate addition of excess amount of KI followed by placing it to attain equilibrium. The obtained amount was determined by performing Iodometric titration versus 0.1 mM Na₂S₂O₃.

Calculation:



Total volume of 0.1 mM Na₂S₂O₃ consumed during titration for Co-NSC8 = 23.5 mL

Volume taken in the flask (0.4 M HCl and excess KI) = 16 mL

On applying the molarity equation:

$$M1 \times V1 = M2 \times V2$$

$$0.1 \text{ mM} \times 23.5 \text{ mL} = M2 \times 16 \text{ mL}$$

$$M2 = 0.146 \text{ mM (I}_3^-)$$

As can be seen in the stoichiometric equation two thio molecules are required for one (I₃⁻), therefore the

concentration of thio would be equal to $\frac{0.146}{2} = 0.073 \text{ mM}$ or $0.073 \times 10^{-3} \text{ mol/l}$

The amount of chlorine evolved or present in the solution = $0.073 \times 10^{-3} \text{ mol/l} \times 71 \text{ g/mol} = 5.1 \text{ mg/l}$ or 5.1 ppm.

Table 5: Iodometric titration for chlorine determination		
Sample	Mean Volume of Na₂S₂O₃ (ml)	Cl₂ evolved* (ppm)
Co-NSC6	43.2	3.2
Co-NSC8	61.6	5.1
Co-NSC9	57.5	4.9

*All the measurements were performed minimum three times at 16 °C

Further, the amount of evolved chlorine was used to calculate the Faradaic efficiency as:

$$Q_{\text{theo}} = \frac{i * t}{nF} = \frac{0.00475A * 50s}{2 * 96500s \text{ A/mol}} = 1.24 * 10^{-6} \text{ mole}$$

Upon converting the obtained value in mol/l considering the 16 ml of volume taken to evolve the chlorine: $0.076 \times 10^{-3} \text{ mol/l}$

The amount of chlorine evolved (Q_{exp}) = 0.073 mol/l or $0.073 \times 10^{-3} \text{ mol/l}$

$$n_{\text{eff}} = Q_{\text{exp}}/Q_{\text{theo}} = 0.073 \times 10^{-3} / 0.076 \times 10^{-3} = 96.05 \%$$

Further the n_{eff} were also evaluated for other variants as tabulated in the table 1.

Table S6; Faradaic efficiency	
Samples	n_{eff} (%)
Co-NSC6	60.5
Co-NSC8	96.05

Co-NSC9	92.1
---------	------

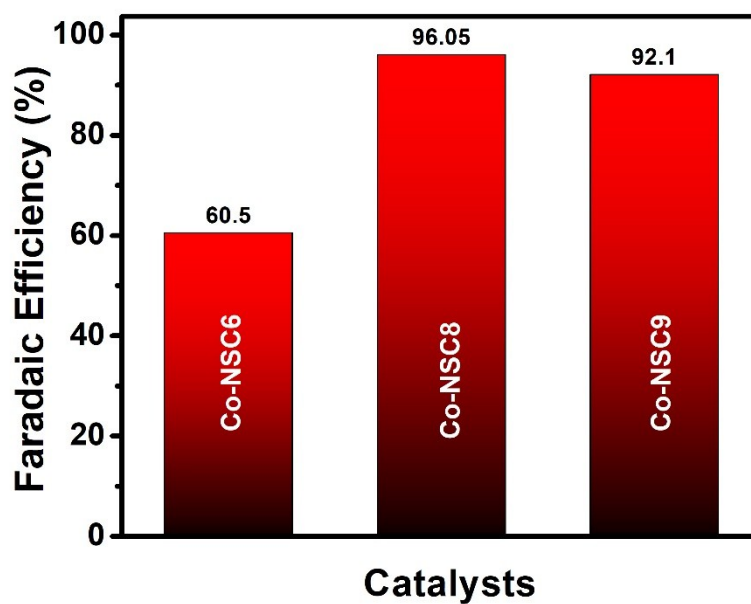


Figure 13. Bar graph represents the obtained faradaic efficiency for all the variants after 50 s of continuous HCl oxidation.

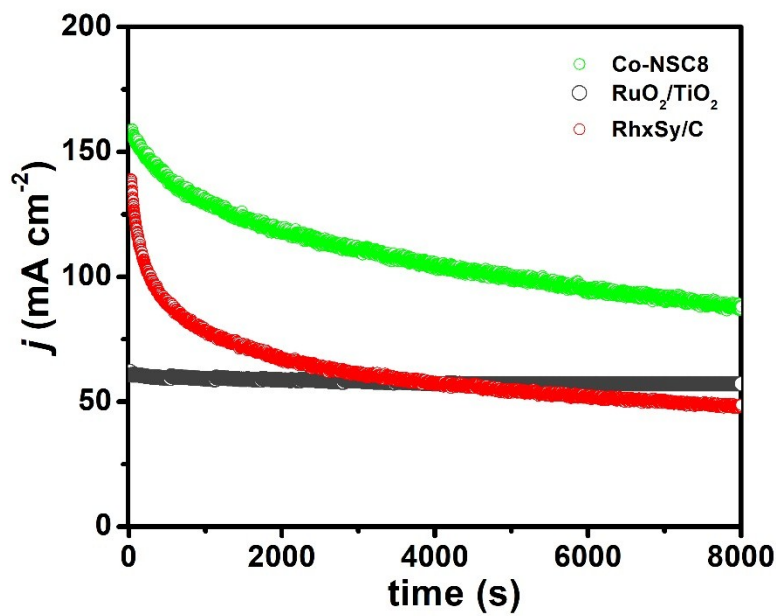


Figure S14. Chronoamperometric stability analysis for each catalysts (Co-NSC8, $\text{RuO}_2/\text{TiO}_2$ and $\text{Rh}_x\text{Sy}/\text{C}$) performed at 1.4 V (vs.RHE) at rotation speed of 500 rpm in 0.4 M HCl.



Figure S15. The microscopic photograph collected after SECM measurements towards ORR under 0.4 M HCl conditions.

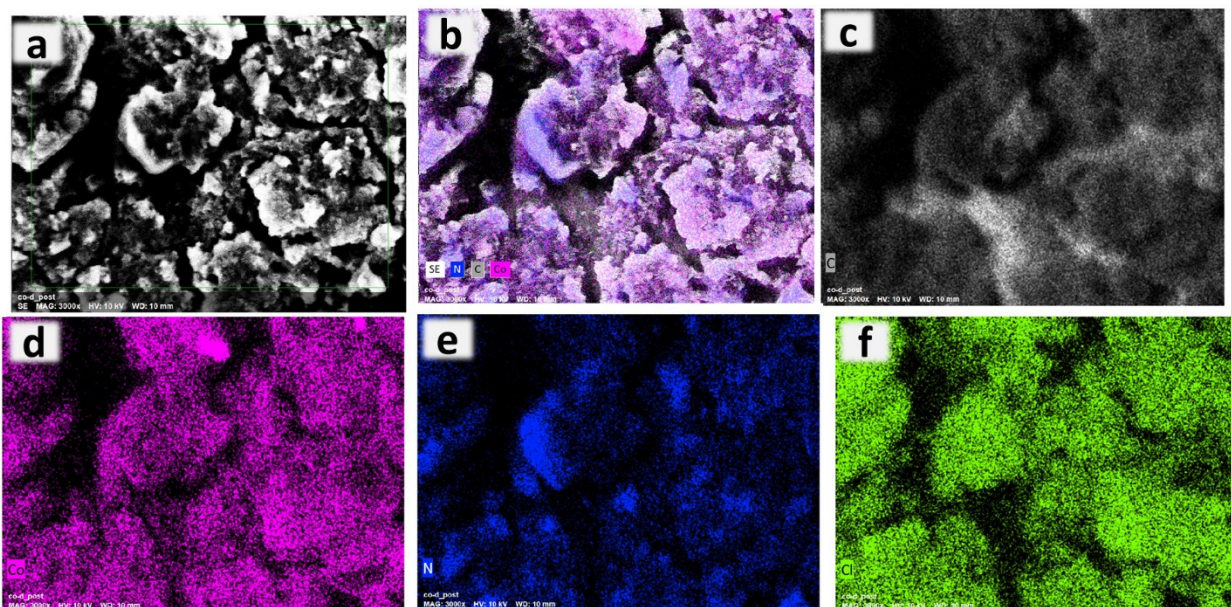


Figure S16. (a) SEM image, (b) superimposable image and (c-f) elemental dot mapping analysis show the presence of (c) Carbon, (d) Cobalt (e) Nitrogen and (f) adsorbed chlorine for Co-NSC8 after 20 h of chrono-stability analysis in 5 M HCl.

References:

1. Osunlaja, A.; Ndahi, N.; Ameh, J., Synthesis, physico-chemical and antimicrobial properties of Co (II), Ni (II) and Cu (II) mixed-ligand complexes of dimethylglyoxime-Part I. *Afr. J. Biotechnol* **2009**, *8*.
2. Singh, V.; Adhikary, S. D.; Tiwari, A.; Mandal, D.; Nagaiah, T. C., Sustainable Non-Noble Metal Bifunctional Catalyst for Oxygen-Depolarized Cathode and Cl₂ Evolution in HCl Electrolysis. *Chem. Mater.* **2017**, *29*, 4253-4264.
3. Kibsgaard, J.; Tsai, C.; Chan, K.; Benck, J. D.; Nørskov, J. K.; Abild-Pedersen, F.; Jaramillo, T. F., Designing an improved transition metal phosphide catalyst for hydrogen evolution using experimental and theoretical trends. *Energy Environ. Sci.* **2015**, *8*, 3022-3029.
4. Fei, H.; Dong, J.; Arellano-Jiménez, M. J.; Ye, G.; Kim, N. D.; Samuel, E. L.; Peng, Z.; Zhu, Z.; Qin, F.; Bao, J., Atomic cobalt on nitrogen-doped graphene for hydrogen generation. *Nat. Commun.* **2015**, *6*, 8668.
5. Beck, J.; Hilbert, T., Ein, altes 'Rhodiumsulfid mit überraschender Struktur: Synthese, Kristallstruktur und elektronische Eigenschaften von Rh₃S₄. *Z. Anorg. Allg. Chem.* **2000**, *626*, 72-79.

